Chapter 5

Characterizing High Mass Galaxy Detections in CHILES

5.1 Introduction

Neutral hydrogen (HI) plays a central role in both driving and regulating star formation, and therefore its content in galaxies is vital to understanding galaxy formation and evolution. The HI content in any given galaxy is an indicator of the complicated interplay between processes that either deplete it (like supernovae), or replenish it (like mergers with gas-rich galaxies). Measuring the HI in galaxies and seeing how it varies with redshift or environment can provide insights into the physics of galaxy formation and test predictions of theoretical models.

There are several models and simulations of galaxy formation and evolution based on the Λ-cold dark matter (ΛCDM) cosmology being explored and refined (e.g., Lagos et al. 2011 ; Davé et al. 2013; Baugh et al. 2019). The two techniques most used to study galaxy formation are hydrodynamical simulations and semi-analytical models, where the first follows the evolution of both the dark matter and baryons

simultaneously, while the second evolves the baryons in a pre-calculated dark matter background, from a set of preliminary assumptions (Blyth et al. 2015). Simulations make predictions about the behavior of the HI content in galaxies at different redshifts and environments. For example, models tested by Kim et al. (2013) predict that the relation between the HI mass and the stellar mass of galaxies will provide additional constraints on the form of ionizing feedback. However, to obtain better limits for these models, HI 21 cm observations are needed to understand how neutral hydrogen behaves in different environments and across redshifts. Unfortunately, HI observations are limited outside the local Universe, due to the faintness of HI emission and the technological limitations of existing facilities to observe at higher redshifts (beyond $z \sim 0.25$) without needing incredibly long integration time and the existence of radio frequency interference (RFI) at those frequencies. More observations of HI in galaxies at different redshifts and environments are necessary to deepen our understanding of this.

The HI content of galaxies in the local Universe and inside of different environments has been explored by wide area HI surveys such as the HI Parkes All-Sky Survey (HIPASS; Meyer et al. 2004), which detected more than 5500 galaxies out to a velocity of 12700 km s^{-1} in the southern sky, and the Arecibo Legacy Fast ALFA (ALFALFA) survey (Giovanelli et al. 2005; Jones et al. 2018), which detected $\sim$ 31500 sources out to a velocity of 18000 km s^{-1} in 7000 deg^2 of sky. However, studies about the change in HI content in galaxies with respect to redshift are more limited due to the difficulties of detecting HI in emission as noted earlier. An example of one that looked at higher redshift ranges is the Blind Ultra Deep HI Environmental Survey (BUDHIES; Verheijen et al. 2007) which observed HI between $z = 0.16$ and $z = 0.22$ around two clusters using the Westerbork Synthesis Radio Telescope and detected a total of 159 galaxies inside the survey volume.

In addition to these, there are many next-generation surveys of HI being de-

veloped or planned at this moment, such as the Widefield ASKAP L-band Legacy All-sky Blind surveY (WALLABY, Koribalski et al. 2020), which is planned to map the southern sky and expected to detect around half a million galaxies in HI using the widefield, high-resolution capability of the Australian Square Kilometer Array Pathfinder (ASKAP) out to a redshift of $z \sim 0.26$, or the Looking at the Distant Universe with MeerKAT Array (LADUMA, Blyth et al. 2016), a very deep HI survey of 3424 hr that will search for galaxies out to $z \sim 1.4$ at the single pointing at RA = 3^h30^m, Dec = $-28°$, using the South African Meer-Karoo Array Telescope (MeerKAT).

The COSMOS HI Large Extragalactic Survey (CHILES) is an HI survey with the VLA which is imaging, for the first time, HI over a contiguous redshift range from $z = 0$ to $z = 0.5$. This is a large project with many international collaborators, led by Jacqueline van Gorkom at Columbia University. This survey observes a single pointing in the Cosmic Evolution Survey (COSMOS; Scoville et al. 2007) field for 1000 hours. COSMOS is a multi-wavelength deep survey that covers a two square degree region centered at RA = $10^h00^m28.6^s$, Dec = $+02°12'21.0''$, which has been studied by many different telescopes in a variety of wavelengths. Observing in this field allows us to take advantage of the extensive ancillary data available. The specific CHILES pointing within the COSMOS region was chosen to avoid bright radio continuum sources close to the field. In addition to exploring the range of redshifts, the CHILES pointing also intersects different environments, such as large-scale galaxy over-densities at several redshifts (at $z = 0.12$, $z = 0.19$, $z = 0.37$) and voids between these. CHILES has published the detection of the highest redshift galaxy to date in HI emission, a gas rich spiral at $z = 0.376$ (Fernández et al. 2016) using images made from the first 178 hours of the survey (referred to as 'Epoch 1').

While CHILES has finished observing, the data processing of the entire survey is still in progress, and at this point we have made images including only the first 300

hours of the survey (Epochs 1 and 2), which are the ones used in this chapter. We expect the final image to have a reduced noise down to 0.55 times the one in the current image, with exceptions where the RFI makes it very difficult to obtain any useable information (See Figure 5.1). We discuss the predicted impact this will have over the detection limits and completeness of the survey in Sections 5.4 and 5.5

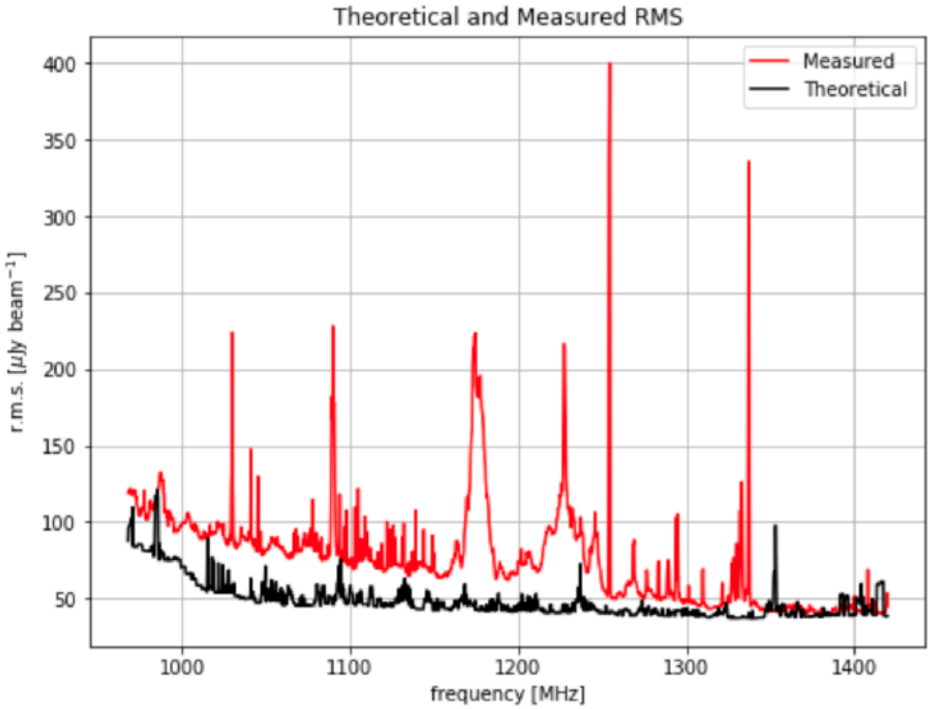

Figure 5.1: The measured rms noise for a naturally weighted cube and the theoretical rms noise calculated by the number of visibilities present in each 250 kHz channel. This is image is taken from an internal CHILES memo written by Nicholas Luber.

The HI mass function (HIMF) describes the intrinsic distribution of galaxies in the Universe as a function of their HI mass, and is crucial to better understand galaxy formation and evolution. This function, which has been derived for the local Universe many times in existing HI surveys, such as HIPASS (Zwaan et al. 2005) and ALFALFA (Jones et al. 2018), has been found to be fit well by a Schechter function

(Schechter 1976), and is well defined in Section 1.4.2.

The three parameters that define the shape of this function are the normalization (Φ^*), the power law exponent, called the low-mass slope (α), and the 'knee' mass ($M_\star$), where the function changes from the power law to the exponential decline. Considering cosmological simulations that now include gas and baryonic processes (e.g. Crain et al. 2015), HI is one of the most sensitive baryonic components to galaxy interactions and hard radiation fields, which means that the HIMF, and how it varies with environment or redshift, are important constraints for the galaxy populations in these simulations (Jones et al. 2018).

In particular, we can see that simulations for galaxy formation and evolution predict different shapes for the HIMF at different redshifts and environments (e.g. Figure 5.2). Additionally, Kim et al. (2013, 2015) show how different star formation laws affect the shape of the local HIMF. With additional information about the shape that the HIMF takes at different redshifts, these simulations can be used to better understand the physical processes behind galaxy formation (Kim et al. 2015).

Given that CHILES will be detecting only high-mass galaxies at higher redshift (see Figure 5.3), the part of the HIMF that we will be able to explore with this survey is how the high-mass end of the function changes (or does not) with respect to redshift. With a good characterization of the detection limits and completeness of the survey, the detections (or lack thereof) of high-mass galaxies will at the very least be able to tell us if shape of the high-mass end of the HIMF has changed at higher redshift, and if that change falls within the predicted values.

The rest of this chapter is organized as follows:In Section 5.2 we describe the observations, data processing and imaging of the survey. Section 5.3 describes the predictions of HI mass of galaxies from existing multi-wavelength data, and how these were used to predict the number of galaxies that will be detected in this survey.

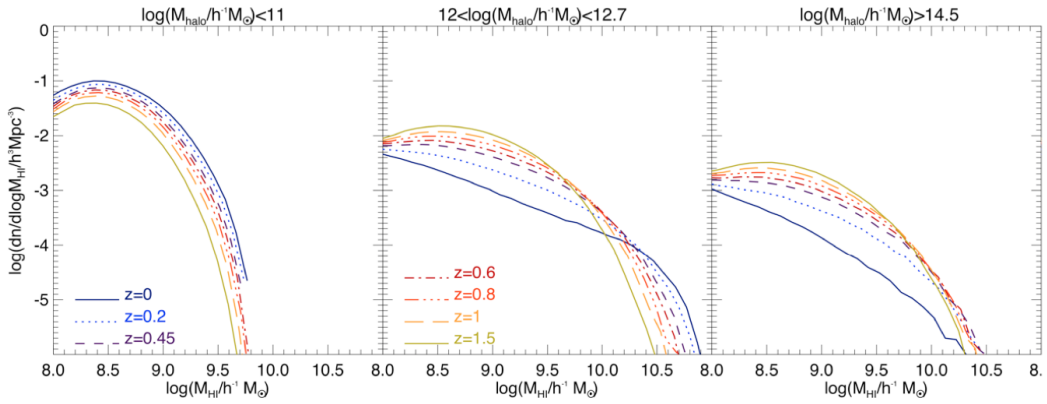

Figure 5.2: Predictions from the semi-analytical models of Lagos et al. (2012) that show the HIMF at different redshifts and halo masses. Halo mass bins correspond to field (left panel), group (middle panel), and cluster (right panel) environments. Halo masses can be used as environmental parameters, such as in Weinmann et al. (2006) or Wetzel et al. (2012). The figure is taken from Blyth et al. (2015).

Section 5.4 describes the artificial galaxies which were made to test the detection limits and completeness of the survey. Section 5.5 explores the completeness of the survey, using the automatic source finding tool SoFiA (Serra et al. 2015). Finally, the conclusions are presented in section 5.6.

5.2 CHILES Data

This section will explore the process of obtaining, calibrating and creating spectral cubes in the CHILES survey. Section 5.2.1 describes the observations, Section 5.2.2 describes the data reduction process, and Section 5.2.3 explains how the data cubes were made.

5.2.1 Observations

CHILES observed a single pointing at RA = $10^h01^m24^s$, Dec = $+02°21'00''$ in the COSMOS field for 1000 hours, using the L-band receiver of the Karl G. Jansky Very Large Array (VLA) in B-configuration. The half-power width of the synthesized beam is $\sim 5''$ at 1.4 GHz, and the half-power width of the primary beam of the VLA is $\sim 32'$ at this frequency. The data used for this chapter were the first 300 hours of the survey ($\sim$ 237 hours on source), taken between 2013 and 2015, which combines Epoch 1 (the first 178 hours) and a portion of Epoch 2 (the next 122 hours; the full Epoch is 210 hours). The L-band receiver has a nominal frequency range of 1 - 2 GHz, and an actual frequency range of $\sim$ 940 - 2200 MHz. For this project, we set up the observations to use the frequency range from $\sim$ 940 MHz to $\sim$ 1430 MHz, which allows CHILES to try and detect 21 cm HI line out to a redshift of $z \sim 0.5$.

This survey used the Wideband Interferometric Digital ARchitecture (WIDAR) correlator of the VLA. We used two of the four 8-bit samplers to obtain dual polarization data with overlap in frequency, and the WIDAR correlator delivered 15 x 32 MHz-wide spectral windows for a 480 MHz contiguous frequency coverage. To mitigate the sub-band edge noise behavior, we used 'frequency dithering', which used different frequency settings offset by a few MHz from each other. The first round of observations (Epoch 1) the settings covered the following frequency ranges: 941-1421, 946 - 1426 and 951 - 1431 MHz. The second round (Epoch 2) used: 947.6 - 1427.6, 952.6 - 1432.6, and 957.6 - 1437.6 MHz. The resulting channel resolution is 31.2 kHz (6.6 km s^{-1} at $z = 0$) after Hanning smoothing.

In order to calibrate the field, each observing session included scans on the flux density scale calibrator J1331+3030 (3C 286), which also served as the bandpass calibrator, and the complex gain calibrator J0943-0819.

5.2.2 Data Processing

The data were reduced with the Common Astronomy Software Applications (CASA) software package (McMullin et al. 2007) using a version of the NRAO VLA continuum pipeline which was significantly modified and tailored for the CHILES spectral line data by the CHILES collaboration. We used RFLAG, one of the automated flagging algorithms available in CASA, without the time averaging or extension options (more details in Blue Bird et al. (2020) and Hess et al. (2019)). We also used masks over regions that have strong RFI, carefully identifying these regions because they changed between Epochs, and applied them to each of the calibrators before calibrating the target data. This pipeline was applied to each data set in the survey, where the data sets were the observations taken on a single night. Most data sets were six hours long, with a few that took data for 3 or 4 hours instead.

After the pipeline was run, we inspected each data set for quality assurance, where experienced members of the team decided if the final results were acceptable or not. If the data did not meet their standards, then we returned to it to manually add flags and rerun the pipeline as necessary, until the final product reached an appropriate level of quality.

5.2.3 Imaging

The image cubes used for this chapter were made using CASA by CHILES collaborators. Each data set was averaged to a frequency resolution of 250 kHz per channel ($\sim$ 50 km s^{-1} at $z = 0$), and then went through two iterations of a UV plane model-based subtraction at two different resolutions (using the CASA task uvsub), in order to subtract the continuum emission from the image. Known continuum sources in the field were specifically targeted for subtraction. The first subtraction used an image the size of the primary beam, while the second one used a radius of 1.5°, with an

angular resolution twice as coarse through a uvtaper. The subtracted data sets were then combined and averaged in the UV plane, before being imaged. Lastly, there was one final linear continuum subtraction done in the image plane per 24 MHz (the size of the cube).

The resulting image cubes have an angular resolution of $\sim$ 6.5″ x 4.5″ at z=0, each one spanning 24 MHz with an overlap of 4 MHz on each end between cubes. The data are imaged with a robustness of 0.8 in the CASA task tclean in order to create images with a well-behaved dirty beam and minimal noise. While natural weighting would have better sensitivity, images made with it have large sidelobes which make this weighting undesirable. Using the robust weighting at this level, we get a sensitivity which is close to natural, but with better behaved noise and point spread function.

5.3 HI Mass Predictions

In order to have an estimate of the number of galaxies that we would eventually detect at the end of this survey, and to create a list of possible detections to perform a targeted search for galaxies, we used the existing ancillary data from the COSMOS field to obtain an estimate of the HI mass for the galaxies in the field with the necessary redshift and multi-wavelength observations.

5.3.1 The HI Mass Estimate

The scaling relation used to estimate the HI mass of the galaxies was derived by Catinella et al. (2012), which relates HI mass to stellar mass, NUV and r magnitudes

as

$$\log\frac{\mathrm{M_{HI}}}{M_*} = a\log\mu_* + b(NUV - r) + c \tag{5.1}$$

where μ_* is the stellar mass surface density, $a = -0.285$, $b = -0.366$ and $c = 2.872$. They used NUV - r as a proxy for the star formation rate per unit of stellar mass, which measures star formation over long timescales. They then found this relation of the gas mass fraction to a linear combination of NUV-r and stellar mass surface density by assuming that the star formation and gas densities are computed over the same region, so that this relation is physically motivated (Catinella et al. 2012). This relation was calculated using a sample of nearby galaxies from the GALEX Arecibo SDSS Survey (GASS), which covered a redshift range from z= 0.025 to z = 0.05.

The numbers used here are for the scaling relation they obtained using galaxies with NUV-r $\leq$ 4.5 mag, which corresponds to most of the galaxies within our sample (out of the 2513 galaxies with spectroscopic redshifts and measurements of NUV, r and stellar mass in the CHILES field, only 342 have NUV - r $\geq$ 4.5, or 14%), and which had an rms scatter in log $\frac{\mathrm{M_{HI}}}{M_*}$ of 0.29 dex.

It is important to take into account two details from the results of Catinella et al. (2012): one, that this relation is meant to be used for statistical purposes and not to be trusted for results in individual galaxies, and two, that this sample did not have many galaxies with very high gas fractions, so predictions for galaxies with very high values of M_{HI} and/or $\mathrm{M}_{HI}/\mathrm{M}_*$ are expected to need additional corrections (e.g., Li et al. 2012).

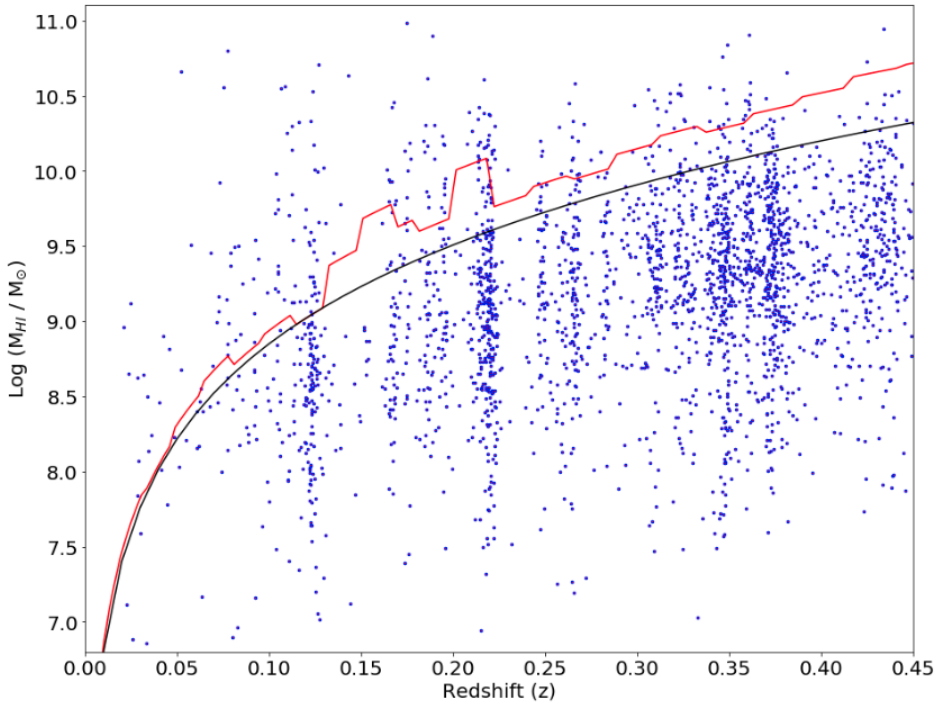

Figure 5.3: The predicted HI masses of the galaxies in the CHILES field (blue circles), as well as the HI mass detection limit of CHILES, as a function of redshift. The red line is based on the measured noise at each 20 MHz frequency range for the first 300 hours of data, while the black line is the original prediction of a detection limit for the entire survey, assuming a galaxy width of 200 km s^{-1} and a S/N of 5.

5.3.2 Predictions in the CHILES Field

In order to make the predictions for the HI mass of galaxies in the observed field, we used the multi-band photometry and redshift information from two catalogs: the G10/COSMOS v05 catalogue[1] and the catalog provided by Laigle et al. (2016). When limited to the galaxies with measurements for: spectroscopic redshift, NUV magnitude, r magnitude, stellar mass and photometric radius, we have a sample of 2513 galaxies in the CHILES field, within a redshift range of$z \leq 0.5$.

[1]http://cutout.icrar.org/G10/dataRelease.php

Using these, we calculate the predicted HI mass of all of these galaxies (Figure 5.3). There are a few limitations to this method of prediction. As said previously, the scaling relation is meant to function statistically and not individually, so while the results of this are a good way to predict the total number of galaxies within a certain mass range, it is not meant to be used to search for specific galaxies. Additionally, this relation is expected to be less accurate with galaxies with higher gas fraction (M_{HI} / M_*) due to the sensitivity limits of GASS, which is a gas fraction limited survey (Catinella et al. 2012). In the higher redshift ranges of this survey, the only galaxies we expect to detect will be the ones with very high HI mass (the theoretical detection limit for a galaxy at the highest redshift, $z = 0.5$, after the full 1000 hours of the survey, is 3 x 10^{10} $M_\odot$). So while we use this HI estimate to get a general estimate of how many galaxies will be above the theoretical detection limit of the survey (see the black line in Figure 5.3), we do not expect to specifically detect every individual galaxy predicted to have a mass large enough to be detected. This detection limit used the criteria described by Giovanelli et al. (2007) for a bivariate signal-to-noise ratio, solved for the HI mass

$$M_{HI} = 2.36 \text{ x } 10^5 \; d^2 \; S/N \; rms \; (2 \; \delta v \; w_{50})^{1/2} \tag{5.2}$$

where d is the distance to a detection in Mpc, w_{50} is the half peak velocity width in km s^{-1} (using 200 km s^{-1}), δv is the velocity resolution of the survey, rms is the noise in Jy, and the S/N is the signal-to-noise of the detected, which is 5 for this prediction. This is usually a good estimate for the detection limits of a survey based on mass, however, it is not perfect. The capability of detecting a galaxy depends also on velocity width, and it is possible to detected lower mass galaxies when they have higher inclinations, and to fail to detected galaxies which were predicted, at lower inclinations.

Additionally, we have to remember that the scaling relation used was based off of data from GASS, which covered a nearby redshift range from z= 0.025 to z = 0.05 (Catinella et al. 2010). There is no guarantee that this trend is valid at higher redshifts, or in different environments; in fact, one of the motivations behind the CHILES survey was to obtain an understanding of how the HI content of galaxies changes with respect to these variables. Moreover, at the higher redshifts we will have to consider that the rest wavelengths will be significantly shifted, and so we should apply K-corrections to obtain the equivalent values. While this has not been calculated for the work in this chapter, we will implement it in future versions of these predictions.

Finally, there is a limitation on the existing observations inside of the COSMOS field. The original scaling relation in the Catinella et al. (2012) paper used a stellar mass surface density based on the z-band radius of the galaxies, but we were unable to use the same measurements for the galaxies in the CHILES field, since we only have this value for $\sim$ 400 galaxies with existing redshift values. Instead, we chose to use another optical radius (from the HST F814W filter, at Λ = 813 nm). According to results from Lange et al. (2015), the difference in the half-light radius from a z-band measurement to a 813 nm measurement is less than 1%. When we compared the z-band radii from the 400 galaxies to the HST F814W filter, we found that these values varied greatly, where the HST radii measured 0.2 to 5 times as large as the z-band radii. The reason for this is the difference in the definition of the radius; the HST radius is the half-light radius, while the z-band radius for these 400 galaxies is the Petrosian radius[2]. In the end, we decided to use the HST radii, which we had far more of, but the value of the radius to be used here could give us significantly

[2]The Petrosian radius is a distance-independent radius measurement for a galaxy. It is defined as the radius where the integrated intensity of light within said radius is equal to a chosen constant multiplied by the average intensity of light within the same radius (Petrosian 1976). For example, the SDSS photometric pipeline chose that constant to be 0.2.

different results for our predictions.

We also include a detection limit based on the measurements of the noise for each 20 MHz cube used in this chapter (the red line in Figure 5.3). This was calculated in the same way as the theoretical 1000 hour detection limit (Equation 5.2), but for the different noise levels measured in each cube.

These estimated HI masses for the galaxies in the CHILES field result in a prediction that once the survey is complete, we expect to find 275 galaxies. At the current stage of the survey, with the 300 h cubes and predictions, this number is down to 131.

Using the predicted HI masses, we also created the HIMF using the galaxies we predict would be detected, both at the theoretical limit after the full survey, and using the measured noise levels of the first 300 h of the survey (Figure 5.4). In order to calculate the HIMF, we used the $\Sigma\ 1/\mathrm{V}_{max}$ method (Schmidt 1968). Each galaxy is weighted by the maximum volume (V_{max}) in which it can be detected, and the value of the HIMF for a particular mass bin is determined by adding up all the weights in it. We fit each distribution with a mass function described by Equation 1.1. For more details, see Section 4.6.

The shape of the HIMF from the predicted galaxies follows what we would expect to see in the case of the predictions for the full survey (the blue line in Figure 5.4), which suggests that these predictions are at the very least good enough to recreate a sample that mimics the general observed shape of a HIMF. However, both of these fits fail to pass through a lot of the points in the mass range from $\log(\mathrm{M}_{HI}/\mathrm{M}_{\odot}) = 9.5$ to 10.2.

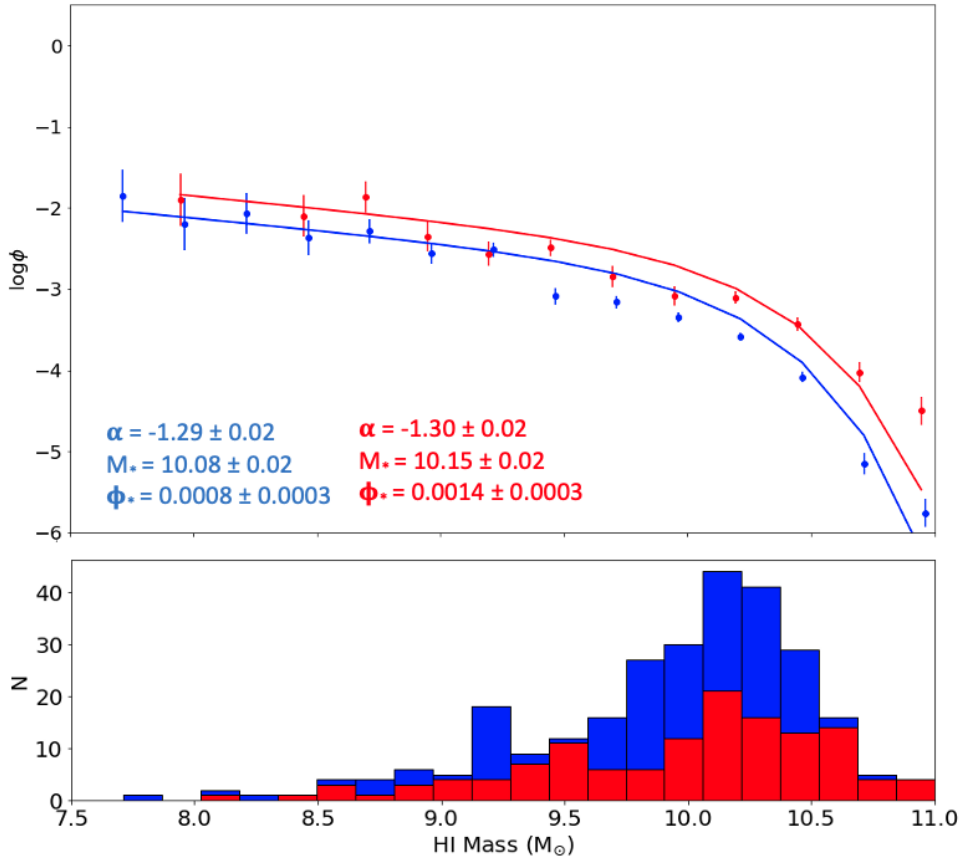

Figure 5.4: The HIMF measured using the predicted HI masses of the galaxies in the CHILES field. At the bottom is the histogram describing the number of galaxies in each mass bin we predict will be detected. The red corresponds to the predictions from the first 300 h of the survey, while the blue corresponds to the predictions for the full 1000 h.

5.4 Artificial Sources and Predicted Galaxies

5.4.1 Creation of Artificial Sources

As can be seen in Figure 5.3, the real behavior of the noise in the CHILES survey is far more complicated than the original, theoretical prediction. In order to better

understand the limits of the survey, and the detectability of sources both by eye and by artificial source detection (more on this in Section 5.5), artificial sources were made and added into the existing cubes, where their detection could be tested.

These artificial sources were made using the Tilted Ring Fitting Code (TiRiFiC), which is a program that constructs simulated spectroscopic data cubes of rotating galactic disks (Józsa et al. 2007). To create an artificial galaxy, a target HI mass is chosen, and then the parameters for the TiRiFiC program were derived to physically correspond to a galaxy of that mass. Additionally, because of the distances involved at the higher redshifts, the HI formulae used were based on the formulae described by Meyer et al. (2017), which use frequency rather than velocity. In this way, the HI mass of any given galaxy is

$$\left(\frac{\mathrm{M_{HI}}}{h_c^{-2}M_\odot}\right) \approx 49.7 \left(\frac{D_L}{h_c^{-2}Mpc}\right)^2 \left(\frac{S}{JyHz}\right) \tag{5.3}$$

where D_L is the luminosity distance and S is the flux, in units of Jy Hz.

The important variables needed for making the artificial galaxy are:

- Radius: using the HI size-mass (D_{HI} - M_{HI}) relation of galaxies, which finds a relation between the HI mass and the diameter of the HI disk, defined at a surface density of 1 $\mathrm{M}_\odot\mathrm{pc}^{-2}$ (Wang et al. 2016), we calculate the radius of the artificial galaxy after choosing the target HI mass. Wang et al. (2016) describe this relation, with D_{HI} in units of kpc and M_{HI} in units of $\mathrm{M}_\odot$, as

$$\log D_{HI} = 0.51 \log \mathrm{M}_{HI} - 3.32 \tag{5.4}$$

- HI surface brightness: described as the HI flux per area, in units of

Jy km s^{-1} $arcsec^{-2}$ as an input. We use the expected HI flux for a galaxy of the chosen HI mass, size and distance.

- Rotation velocity: we use a simple estimate which scales with the HI mass, taken from Chakraborti & Khedekar (2011), who found estimates for the rotation velocity of galaxies by comparing measured HI masses to inclination-corrected HI velocity widths, where the rotation velocity is assumed to be half of that value. This scaling relation is

$$M_{HI} \propto w^{2.36} \tag{5.5}$$

where w is the inclination-corrected velocity width at 20% of peak flux. The results of these values were final velocity width measurements from ~ 0.4 MHz (across two spectral channels) to ~ 2.3 MHz (across 10 channels), within the inserted galaxies of masses between $\log (M_{HI}/M_{\odot}) = 7.0$ to $\log (M_{HI}/M_{\odot}) = 11.0$.

In addition to these variables, we choose the location of the galaxy in the cube by specifying the Right Ascension, Declination, and central frequency. The inclination of each galaxy can be varied at will, and a different parameter for inclination was chosen for both uses of artificial galaxies in this chapter (See the rest of this Section, and Section 5.5). The resulting galaxies are created to match the resolution of the cubes in which they will be inserted.

As a final modification to the artificial galaxies to better predict the possible detections, corrections were made to the total flux of the galaxy corresponding to the primary beam corrections that would be applied to the VLA data. Before each galaxy was added to the original cube, its flux was adjusted by a factor determined by the distance of the center of the artificial galaxy to the center of the field, corresponding to the loss of sensitivity which would be measured at that position in the survey.

5.4.2 Testing Observations with Predicted High-Mass Galaxies

Another use we found for the predicted HI masses calculated for the COSMOS galaxies in the CHILES field described in Section 5.3 was to use them to understand the noise environment of the survey, despite the fact explained earlier about how the predictions for the HI masses of the existing galaxies are not meant to be used to find individual galaxies. We selected the galaxies with very high estimated HI masses (above 2.5 x 10^{10} $M_{\odot}$) and within a radius of 25′ from the center of the field, which turned out to be 42 galaxies in the frequency range from 1000 to 1420 MHz. We decided to exclude the cubes from 951 - 1000 MHz from this search due to unrelated difficulties in working with them. We then looked by eye to see if the expected galaxy could be found. In addition to this, we created artificial galaxies at these positions using the predicted HI mass, using an inclination of 45° for all inserted galaxies, and tried to find them by eye in the same manner, to quantify if such a galaxy would have been detected, and to see if the predictions were true to reality.

Table 5.1 presents the measured and derived parameters of these 42 galaxies in the columns described below:

Column (1) – The COSMOS ID number of the galaxy;

Columns (2) *and* (3) – Equatorial coordinates (J2000) of the galaxy position;

Column (4) – Central frequency of the galaxy's HI signal;

Column (5) – The predicted HI mass of the galaxy;

Column (6) – The predicted HI mass of the galaxy, taking into account the primary beam correction and how far it is from the center of the pointing;

Column (7) – Identification of how the galaxy was detected, if at all. 'o' means

that the original galaxy was detected in the CHILES image cube. 'a' means that the artificial galaxy, of the predicted size, was detected in the modified CHILES image cube. 'n' means that neither one of these were detected.

Table 5.1: Summary of individual galaxies searched.

COSMOS ID	**R.A.**	**Dec.**	**Freq**	$M_{predicted}$	$M_{PBcorrected}$	**Detection**
	$^\circ$	$^\circ$	MHz	$M_\odot$	$M_\odot$	
(1)	(2)	(3)	(4)	(5)	(6)	(7)
1433889	150.38	2.52	1021.1	10.40	10.33	n
753269	150.25	2.04	1028.5	10.65	10.37	n
1464603	150.21	2.47	1036.8	10.48	10.40	n
1406396	150.43	2.54	1042.9	10.57	10.47	n
780600	150.10	2.02	1042.9	10.51	9.99	n
1658388	150.34	2.65	1043.6	10.91	10.66	n
788184	150.17	1.98	1043.6	10.44	9.93	n
1221790	150.22	2.30	1043.6	10.41	10.36	n
521691	150.37	1.94	1044.4	10.46	9.96	n
1003543	150.15	2.23	1045.2	10.47	10.32	n
1626760	150.50	2.69	1052.9	10.84	10.48	n
934268	150.58	2.19	1052.9	10.45	10.27	n
1396147	150.50	2.61	1054.5	10.54	10.33	n
1401798	150.47	2.57	1055.3	10.76	10.65	a
1001752	150.17	2.24	1060.8	10.56	10.49	n
1400086	150.50	2.59	1072.8	10.50	10.31	n
736456	150.42	1.98	1073.6	10.57	10.18	n
746526	150.39	2.08	1073.6	10.51	10.34	n
741886	150.33	2.12	1074.4	10.52	10.41	n

Continued on next page

Table 5.1 – continued from previous page

COSMOS ID	**R.A.**	**Dec.**	**Freq**	$M_{predicted}$	$M_{PBcorrected}$	**Detection**
	°	°	MHz	$M_\odot$	$M_\odot$	
(1)	(2)	(3)	(4)	(5)	(6)	(7)
991528	150.32	2.14	1077.7	10.52	10.42	n
725068	150.43	2.06	1077.7	10.46	10.23	n
726954	150.42	2.06	1079.3	10.40	10.17	n
1000527	150.09	2.25	1083.4	10.42	10.22	n
705338	150.60	2.04	1085.1	10.47	10.00	n
1248253	150.02	2.44	1087.6	10.54	10.23	n
961560	150.54	2.17	1094.3	10.44	10.26	n
1193049	150.47	2.33	1121.9	10.58	10.52	n
724052	150.47	2.08	1124.6	10.45	10.17	n
1221492	150.32	2.46	1167.1	10.61	10.53	a
998606	150.20	2.26	1170.0	10.42	10.29	n
974598	150.36	2.25	1194.6	10.90	10.81	a
1033735	150.05	2.20	1197.6	10.62	10.15	n
1438603	150.37	2.48	1208.8	10.98	10.86	n
991411	150.33	2.14	1216.1	10.46	10.23	n
1432217	150.23	2.53	1217.1	10.43	10.19	n
1425963	150.26	2.58	1242.7	10.63	10.33	n
950723	150.47	2.24	1260.3	10.71	10.52	a
1484742	150.02	2.50	1281.9	10.56	9.88	n
1452928	150.19	2.55	1283.1	10.55	10.19	a
1428287	150.25	2.56	1317.6	10.80	10.44	a
1437568	150.31	2.48	1321.3	10.56	10.34	o
950685	150.40	2.24	1350.2	10.66	10.24	a

After searching the 42 galaxies by eye, we identified only a single possible detection. While this might seem to be inconsistent with the detection limit we set for Figure 5.3, it is important to remember that we are only considering estimated HI mass values, and at this point we cannot say whether the lack of detection is due to them being of a different mass in reality or because we failed to detect them despite the calculated detection limit. In order to study this, we then added artificial sources at the exact position and frequency as the COSMOS galaxies, with the predicted HI masses (in the frequency range from 1000 MHz -1351 MHz, see Table 5.1). After considering the primary beam corrections, we expected to detect 25 of them. When they were searched one by one, by eye, 7 were detected. Because we already knew where an artificially inserted source was, however, there was an inherent bias in looking for the galaxy, and so we came up with another criteria to consider it a detection. The cubes were searched channel by channel by looking for signal above 3σ of the noise across the channels we knew the artificial galaxy inhabited, and we classified it as a detection if we could see it across at least three channels. However, even considering this, most of the added galaxies went completely undetected. See Figure 5.5 for an example of an artificial galaxy inserted into a higher redshifts, projected into an HST image.

As we can see in Figure 5.5, as well as from the results from Table 5.1, the noise environment of CHILES is making it difficult to predict well what we will be able to detect. The problems can be split into two: there is a large frequency range with severe RFI that dramatically increases the noise and detection limits inside of it, and in the lower-frequency cubes with better noise, this noise turns out to be non-Gaussian (see Figure 5.5).

The frequency range we identify as having known bad RFI is between 1170 - 1300 MHz (see Figure 5.1), and 10 of the galaxies we searched for are in this range.

Of these, we detect only 3 of the inserted artificial galaxies, despite 9 of them being theoretically massive enough to be within the detection limit of this frequency range. This is due to large stripes of noise that completely wipe out most signals which cause many of the inserted galaxies to disappear into very high local noise.

In the case of the cubes from 1000 - 1170 MHz, the problem we have is that, despite not having the same devastating regions of RFI, the noise is non-Gaussian. As a result of this noise environment, part or the whole of a galaxy which should be detected may fall into a region where the noise has large positive or negative dips, and the signal is completely lost inside this region (see Figure 5.5). Likewise, nearby noise spikes far larger than the signal of the galaxy itself could make it difficult to convince someone searching the image cube that a candidate galaxy is real.

In the higher frequency cubes, we do not run into either of these problems. All galaxies inserted into the frequency range 1282 - 1360 MHz were found, as was a single real detection, which had a much smaller mass than the predicted HI mass of that galaxy.

As a result, we are not able to detect most galaxies, especially at the higher redshifts, even when we artificially insert galaxies we know to have an HI mass far above the detection limit we had originally calculated.

5.5 Completeness

To estimate the completeness limit of the CHILES survey, both at its current state and in the future once we have an image cube of the entire survey, we decided to use artificial sources to test the automatic source finding algorithm SoFiA (the Source Finding Application; Serra et al. 2015) which is being used by many CHILES team members to find new galaxies in this survey. SoFiA is a modular GUI based

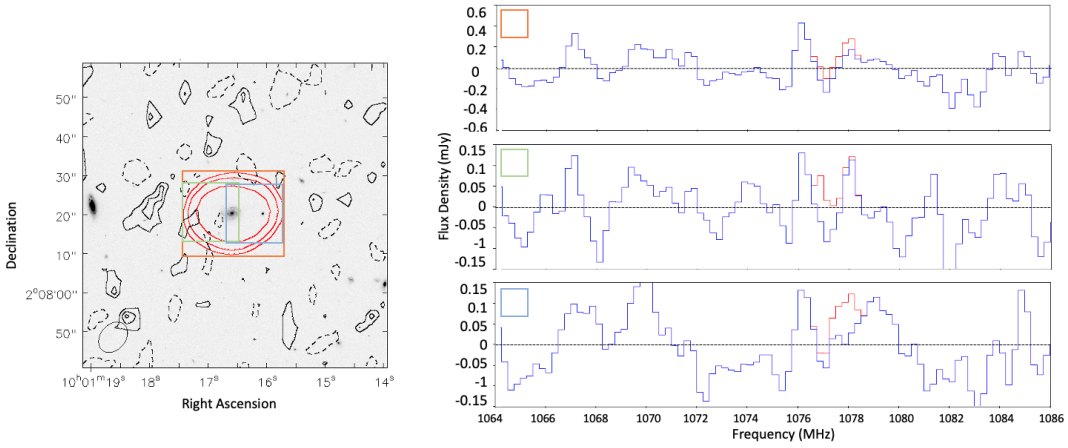

Figure 5.5: Galaxy 991528 in the background HST image, with the black contours showing the moment 0 map of the CHILES cube with the inserted artificial galaxy at -2x, 2x, 3x and 5x of the rms noise, and the red contours representing the outline of the artificial galaxy before being inserted. All boxes indicate where the spectral profiles were measured, and the HI profiles on the right shows the integrated flux from inside those box, where the blue is the spectrum of the original cube, and the red shows the added flux of the artificial galaxy.

application with a collection of algorithms in a single pipeline. It takes in FITS files as input and outputs several catalog formats and data products, including moment maps.

We took each of the 24 MHz cubes of the survey individually and calculated the comoving volume contained within each, considering only the region inside of a radius of 21′ from the center of the field, which is within the FWHM of the beam (32′ at 1420 MHz). Using this volume and an existing fit of the HIMF (here we used the results from the total 100% of the ALFALFA survey calculated by Jones et al. (2018)), we predict how many galaxies within certain mass bins would be expected to exist within this volume, and generate that number of artificial sources, which are spread across the CHILES cube with arbitrary inclinations and positions. All galaxies with a mass that is at least one mass bin below the detection limit for each

cube were added, in order to test the more marginal cases. The flux of every galaxy was primary beam corrected. See more details in Table 5.2.

Table 5.2: Summary of inserted galaxies to test for completeness. Frequency ranges marked by an asterisk refer to the cubes which were examined for this Chapter.

Frequency Range MHz	Mass Range $\log(M_{HI}/M_\odot)$	rms noise μJy/beam	added galaxies	found blind	found targeted
951-968	10.4-10.8	108	10		
964-988	10.4-10.8	90	9		
984-1008	10.4-10.8	85	8		
1004-1028	10.4-10.8	69	7		
1024-1048	10.2-10.8	70	32		
1044-1068	10.2-10.8	59	27		
1064-1088	10.2-10.6	60	23		
1084-1108	10.0-10.6	78	60		
1104-1128	9.8-10.6	55	112		
1124-1148	9.8-10.6	53	95		
1144-1168	9.8-10.6	55	77		
1164-1188	9.8-10.6	141	65		
1184-1208	9.6-10.6	62	94		
1196-1220	9.6-10.6	89	83		
1216-1240	9.6-10.6	282	65		
1236-1260	9.4-10.6	102	83		
1256-1280	9.0-10.6	47	131		
1276-1300	9.0-10.4	50	93		
1296-1320	8.8-10.4	36	87		
1316-1340	8.4-10.4	76	93		
1336-1360	8.0-10.2	67	81		
1356-1380*	8.0-10.2	31	36	10	22
1376-1400*	7.0-10.0	31	35	3	15
1396-1420*	6.0-9.4	34	13	2	8

At this point, we decided to focus on the three cubes that covered the least noisy frequency space in the survey, which span the frequency range 1356 - 1420 MHz. This was done in order to go over, in detail, the resulting artificial galaxies by eye as well as with SoFiA, to test both the artificial galaxies as well as the source finding software. Additionally, this was done to test how the frequency range with the best

noise in the survey would stand up to examination (See the frequency range from 1350 - 1420 MHz in Figure 5.1). Starting at the next cube in frequency, 1336 - 1360 MHz, the number of inserted galaxies rose to 81, given the larger comoving volume, and inspecting individual sources both by eye and in SoFiA would become a time-intensive task.

In the future, as discussed in Section 6.2, we will test the rest of the frequency range using a combination of SoFiA and personal inspection. In the cases of galaxies above the theoretical detection limit that SoFiA should detect, but does not, we need to look more closely to understand why. For example, this could be due to the galaxy being inside a noise spike or high RFI region, or else it might be an edge-on galaxy where the emission between both peaks of the galaxy might be obscured by the overall noise. We expect to see a loss of detections given the extreme noise environment in the 1170 - 1300 MHz frequency range discussed in the previous section, as well as the problem with non-Gaussian noise at higher redshifts.

A CHILES collaborator conducted the search for the artificial galaxies injected into these three CHILES image cubes (Blue Bird et al. in prep), and the analysis of that search presented here was done by me. The SoFiA algorithm used for this search was Smooth & Clip (S&C) (Serra et al. 2012). This algorithm searched for emission at multiple resolutions by smoothing the cube in three dimensions with specified kernels. The cube was smoothed at two resolutions in the sky using Gaussian kernels, which were roughly 1.5 and 2 times the synthesized beam, values which were chosen after testing many different smoothing kernels. The cube was then smoothed at multiple resolutions in velocity using boxcar kernels, where the kernels vary depending on the width of the spectrum of the galaxy. At each resolution, a specified relative flux threshold of 3.5 or 4 σ was applied to extract and mark the significant pixels at each scale.

In addition to this, a noise scaling filter was applied in SoFiA along the velocity

axis to normalize the data cube by the local noise level, in order to account for variable noise characteristics (such as RFI) throughout the cube. At each resolution, a specified relative flux threshold was applied to extract and mark the significant pixels at each scale. The final mask was produced through the union of the masks constructed at the various resolutions, and significant pixels were then merged into a final source. A specified maximum separation, defined as the distance between two detected pixels where they are considered part of the same source, was applied. Peaks found within a few pixels in right ascension, declination, and velocity were merged together. Once the pixels were merged into a source, the size of each source was checked in each dimension, and sources falling below a specified minimum separation would be discarded to eliminate spurious detections.

The cubes were first run through SoFiA with a blind search, in which reliability parameters were used to reduce the number of false detections. The reliability was determined by parametrizing both positive and negative detections, where all negative detections are assumed to be noise, and then SoFiA determined what the probability for each positive detection being real. In our case, sources below a reliability of 90% were rejected. The method is explained in detail in Serra et al. (2012). As another limit, a minimum total flux value was set for reliable positive detections. Running SoFiA with these parameters found only the highest mass galaxies, as well as those which were most face-on.

After being searched blindly as described above, the CHILES cubes with inserted galaxies were then run through SoFiA using a targeted search, which used a list of the positions of the artificial galaxies. The targeted search extracted cubelets around specified positions to look for detections. In order to find as many of the target detections as possible, we attempted to optimize the parameters to exclude as many false-positives as possible without sacrificing detections. Unlike the blind search, no reliability parameters were set for the targeted search, because we do not

have to worry about spurious detections when we are looking at a place we know a galaxy to be.

5.5.1 1396 - 1420 MHz Cube

This cube had an overall rms noise of 34 μJy per beam per channel, at a channel width of 50 km s^{-1}, and had a total of 13 galaxies of masses varying from 10^6 $M_\odot$ to 2.0 x 10^9 $M_\odot$. Of these, two were excluded from the search given their size and proximity– they had HI masses of 2.0 x 10^9 $M_\odot$ and 7.9 x 10^8 $M_\odot$ and recessional velocities of 150 km s^{-1} and 420 km s^{-1}, respectively. Both of these galaxies dominate the sky and the search algorithms are not optimized for such extraordinarily large objects. Three more galaxies were cut off at the edges of the cubes in frequency, and were therefore also excluded for this analysis. Of the remaining 8 artificial galaxies, the inserted HI mass range, after primary beam correction, was: 1.8 x 10^6 $M_\odot$ to 2.5 x 10^8 $M_\odot$. The mass detection limit for this cube was 6.4 x 10^7 $M_\odot$, for a galaxy with 150 km s^{-1} velocity width at 5 σ. See Figure 5.6 for details.

Two of the eight sources described above were above this detection limit. When searched blindly by eye, we found 5 sources: 2 real, published galaxy detections, the two artificial galaxies above the detection limit, and an additional artificial one with an HI mass of 1.6 x 10^7 $M_\odot$, which is below the mass detection limit of the cube. When searched blindly with SoFiA, it found four out of the five we detected by eye, and the galaxy not found was the artificial galaxy located outside the half-width of the primary beam. In contrast, using the targeted search, SoFiA found all 8 artificial galaxies, including all those below the detection limit. As noted earlier, the mass detection limit is not perfect: it is possible to detect below it when the velocity width is more narrow (in this case, for galaxies which are more face-on, such as the one the blind search finds below the limit). Additionally, the limit itself can be flawed, since

it is based on real noise measurement of the average rms noise of the cube, but there can be channels of higher noise that make detections almost impossible (such as for very strong RFI), or raise the average noise of a cube where there are some regions of lower noise with proportionately lower detection limits.

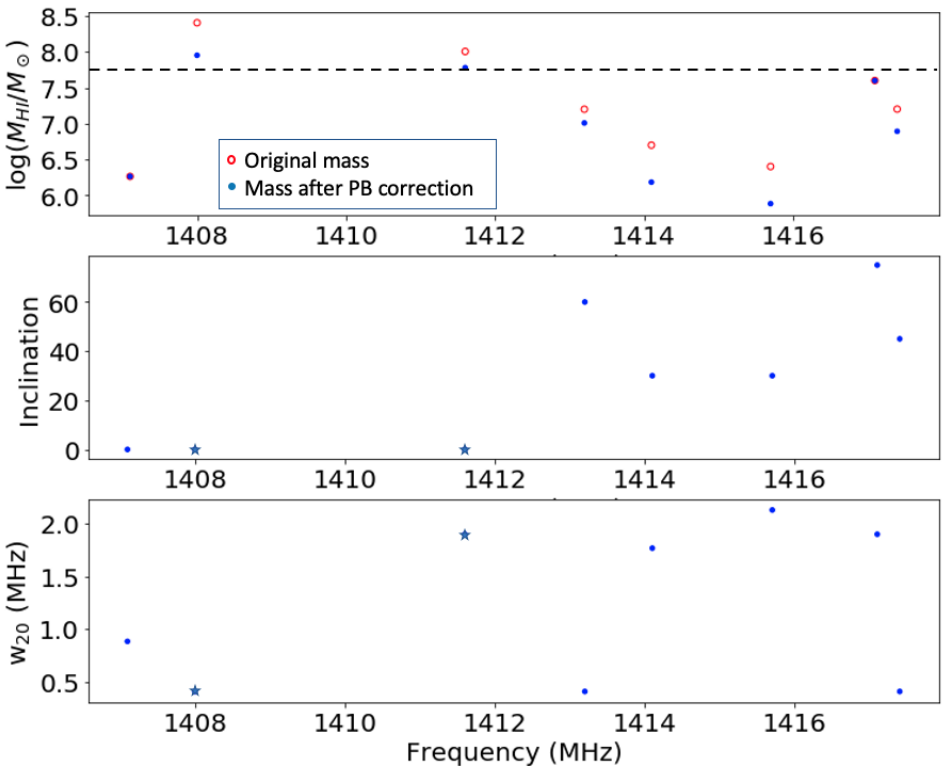

Figure 5.6: The properties of the 8 inserted artificial galaxies in the 1396 - 1420 MHz cube. Top: the HI masses of the inserted galaxies as a function of their frequency. The empty red circles represent the original mass of the galaxy, and the blue dots represent the actual inserted mass after taking into account the position of the artificial galaxy and solving for the primary beam correction. The black dashed line is the measured detection limit for this cube. Note how some galaxies fall below the detection limit due to the primary beam correction. Middle: The inclination of the same galaxies. Bottom: the velocity width of those galaxies. The stars represent the galaxies above the detection limit.

5.5.2 1376 - 1400 MHz Cube

With an overall rms noise of 31 μJy per beam per channel, at a channel width of 50 km s^{-1}, this cube had 35 inserted artificial galaxies with an HI mass range from 10^7 M$_\odot$ to 10^{10} M$_\odot$. One of these was excluded because a majority of it was outside the frequency range of the cube. After applying the primary beam correction to the remaining 34, the mass range for the inserted galaxies was between 9.6 x 10^6M$_\odot$ to 6.5 x 10^9 M$_\odot$. The HI mass detection limit for this cube is 2.0 x 10^8 M$_\odot$, for a galaxy with 150 km s^{-1} velocity width at 5σ. See Figure 5.7 for details.

Eight of these thirty-four artificial sources were above the detection limit after primary beam correction. In addition, there are two real, published galaxy detections in this cube. When searched blindly with SoFiA, we found four galaxies: the three with the highest mass (two which were artificial, and one which was real), and one galaxy above the mass limit that is both face-on, and at the center of the field. In the targeted search, SoFiA found all eight artificial galaxies above the detection limit, as well as seven galaxies below it and the two real galaxies. In the case of the detected galaxies below the detection limit, they either had high inclinations or were close to the field center.

5.5.3 1356 - 1380 MHz Cube

This cube had an rms noise of 31 μJy per beam per channel, at a channel width of 50 km s^{-1}, with a total of 36 inserted artificial galaxies in the mass range from 10^8 M$_\odot$ to 1.6 x 10^{10} M$_\odot$. Of these, two were excluded due to having most of their flux outside of the cube's frequency range. After primary beam correction, the range of masses is 4.3 x 10^7 M$_\odot$ to 1.1 x 10^{10} M$_\odot$. The HI mass detection limit for a velocity width of 150 km s^{-1} and a detection at a 5 σ level in this cube was 4.2 x 10^8 M$_\odot$. See Figure 5.8 for details.

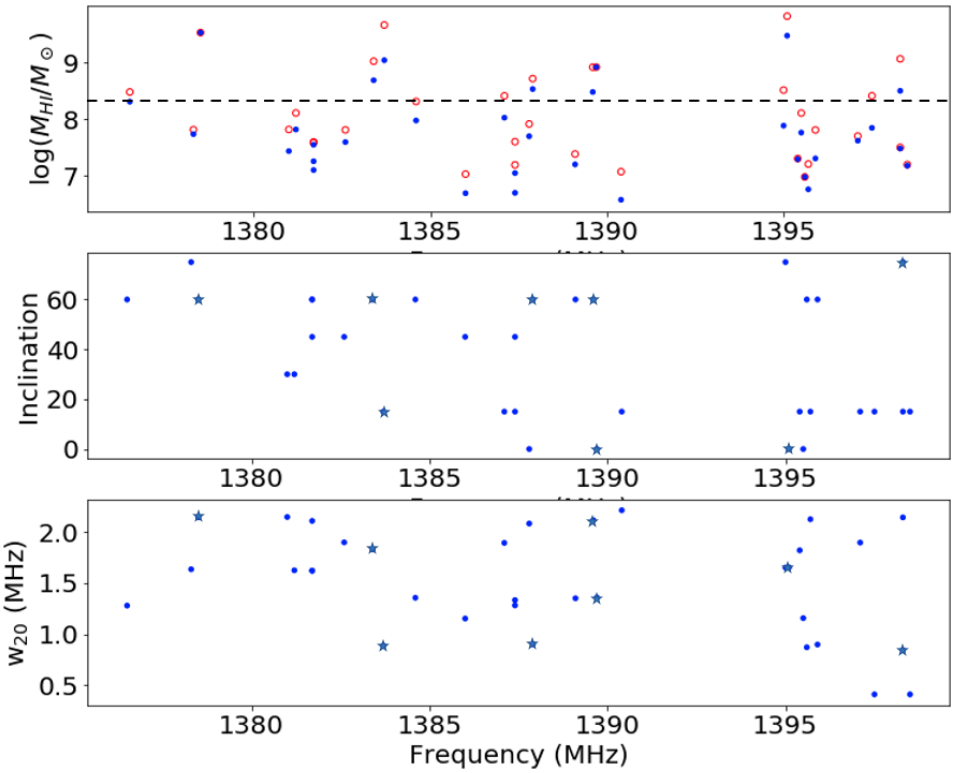

Figure 5.7: The properties of the 34 inserted artificial galaxies in the 1376-1400 MHz cube. Top: the HI masses of the inserted galaxies as a function of their frequency. The empty red circles represent the original mass of the galaxy, and the blue dots represent the actual inserted mass after taking into account the position of the artificial galaxy and solving for the primary beam correction. The black dashed line is the measured detection limit for this cube. Note how some galaxies fall below the detection limit due to the primary beam correction. Middle: The inclination of the same galaxies. The stars represent the galaxies which are above the detection limit. Bottom: the velocity width of those galaxies. The stars represent the galaxies above the detection limit.

Fifteen of the thirty-four analyzed artificial galaxies were above the detection limit after primary beam correction, and there were four real galaxy detections inside the cube. The blind SoFiA search resulted in ten total artificial galaxies: eight which were the highest mass galaxies above the detection limit, with two below that were near the field center and had a face-on inclination. It also found two of the four real

galaxies. The targeted SoFiA search found all fifteen galaxies above the detection limit, as well as seven galaxies below it. In the same way as in the previous cube, the galaxies found below the detection limit either had face-on inclinations or were close to the field center. The targeted search also found all four real galaxies.

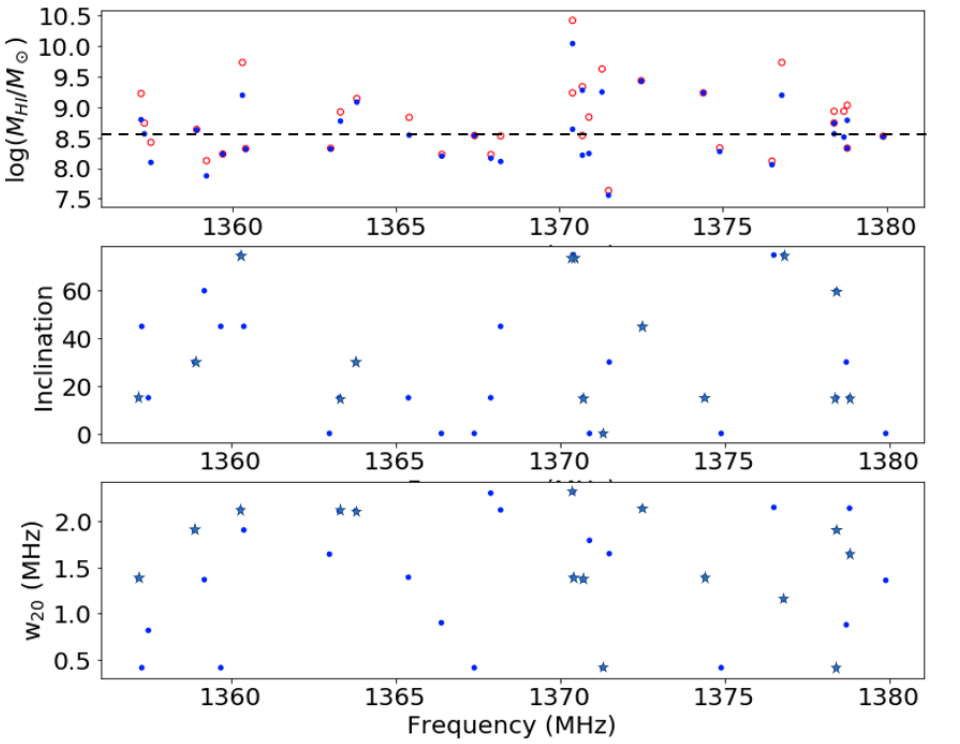

Figure 5.8: The properties of the 34 inserted artificial galaxies in the 1376-1400 MHz cube. Top: the HI masses of the inserted galaxies as a function of their frequency. The empty red circles represent the original mass of the galaxy, and the blue dots represent the actual inserted mass after taking into account the position of the artificial galaxy and solving for the primary beam (PB) correction. The black dashed line is the measured detection limit for this cube. Note how some galaxies fall below the detection limit due to the primary beam correction. Middle: The inclination of the same galaxies. The stars represent the galaxies which are above the detection limit. Bottom: the velocity width of those galaxies. The stars represent the galaxies above the detection limit.

5.5.4 Calculating the Completeness

The results from these tests for the three highest frequency cubes are in agreement with the results from the previous section: the high-frequency cubes of the CHILES survey (above 1300 MHz) behave as expected and most of the galaxies with masses we expect to detect, by eye, are detected in such a way. With respect to the performance of SoFiA, we see vast differences in the blind searches and in the targeted ones.

The SoFiA blind searches are able to detect all of the highest-mass galaxies within a cube, but they struggles to find all of the galaxies which should be within the detection limit, although there is a higher probability of finding a galaxy if it is close to being a face-on source. By contrast, the SoFiA targeted search found all of the detections above the HI mass limit, and many more below this threshold, if the galaxy was close to the center of the field or had a low inclination which would give it a single peak profile, which are easier to detect above the noise.

These results imply that the best way to find all of the galaxies in the CHILES survey would be through a combination of blind searches by eye and with SoFiA, as well as targeted searches in the areas we know there to be a galaxy, in the cases where the exiting COSMOS multi-wavelength data provides a redshift measurement. This is also described in Section 6.2.

Using these galaxies to measure the completeness of the survey for the frequency ranges from 1356 - 1420 MHz is possible (Figure 5.9). We define the completeness of this survey as the fraction of a certain type of galaxy which can be detected in the survey from the underlying distribution of objects down to the detection limit of the survey. We can do a similar analysis as the one done by Hoppmann et al. (2015), where we analyze the ratio of detected galaxies to the number of all galaxies in bins of varying width, while plotting against integrated flux bins.

The results of this show us that the completeness limit for the SoFiA blind

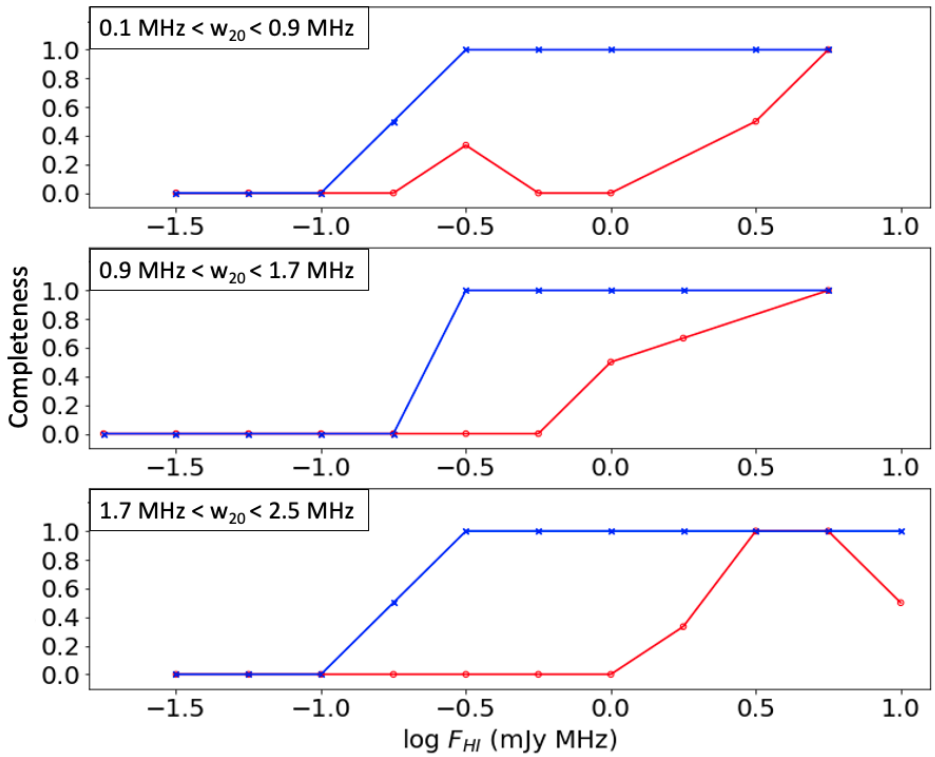

Figure 5.9: 1D slices of the completeness in different bins of frequency width for the frequency range between 1356 - 1420 MHz in the first 300 hours of the CHILES survey, plotted against bins with the integrated flux of each source. Red represents the SoFiA blind searches, while blue represents the SoFiA targeted searches.

searches is much lower than the one for the targeted search. The mentioned frequency widths for the inserted galaxies, 0.1, 0.7, 1.9 and 2.6 MHz, correspond to 21, 190, 360 and 530 km s^{-1}, respectively. For the targeted searches, SoFiA is finding all artificial galaxies with integrated flux above 0.24 mJy MHz (240 Jy Hz), regardless of velocity width. For the blind search, it found most galaxies with a flux above 4.2 mJy MHz (4200 Jy Hz).

However, our current approach to finding the completeness limit has two problems: the low number of galaxies searched, and how many of our high-mass galaxies being close to edge-on because of the random selection of inclinations. This resulted

in highly visible sources with very wide spectral profiles. To get a better estimate for the completeness going forward, the population of galaxies being inserted will have an even spread of velocity widths per mass bin (for every mass bin, we will be inserting the same number of galaxies at different intervals of inclination), and more galaxies in total will be inserted. We will still use the test with the galaxies added in accordance with the HIMF, once the completeness has been determined, to examine how well we are recreating a known HIMF from a sample we control.

5.6 Conclusions

This chapter explored the characteristics of the detection limits and completeness of CHILES, a project carried out with the VLA for a frequency range between $\sim$ 940-1430 MHz. This survey observed the same pointing in the sky, in the COSMOS region, for 1000 hours. We explore the results from image cubes made out of the first 300 hours of the survey. The summary of the results reported here is as follows:

- Out of the 2513 galaxies with previous multi-wavelength information in the CHILES field, we originally predicted that we would detect $\sim$ 300 galaxies in the full 1000 hours of the survey;
- However, the noise environment of the survey, in particular at higher redshifts, make the detection limits more complicated. This has to be fixed before we can get the predicted number of detections. We have not yet found the solution for this problem, but we are working on understanding the source of the non-Gaussian noise in order to get the expected noise levels. The team is also working on better removing the RFI from the data and in subtracting the large side-lobes caused by bright sources away from the field center. Even at

1000 hours, if the noise continues to be non-Gaussian, and these problems have not been solved, detections will continue to be difficult to make. This is not a problem that CHILES alone will have to deal with, as other deep surveys that are probing into higher redshifts are already running into many of the same problems with respect to the RFI environment. The current software is causing a bottleneck in processing the data, as the most common tools for processing spectral data are not equipped to solve any of these problems;

- Out of 42 artificial galaxies searched and/or inserted into frequencies above 1000 MHz, with masses above $\log(M_{HI}/M_{\odot}) = 10.4$, generated across the survey at locations where real galaxies exist, we were able to detect 7 artificial sources and one real source. After considering the reduced flux due to primary beam correction for sources away from the field center, 25 of the 41 inserted sources were above the calculated detection limit.

- SoFiA detected a total of 15 out of 84 inserted galaxies using the blind search (18%), and 45 out of the same 84 inserted galaxies with the targeted search (54%). When considering only the galaxies above the predicted detection limit, the targeted search found 25 out of 25 inserted galaxies (100%) while the blind search found 13 out of the 25 (52%).

- We find that SoFiA is very capable of finding galaxies when the targeted search method is used, but has trouble finding all of the galaxies it is expected to find when used in blind mode. We find that for CHILES in the frequency range 1356 - 1420 MHz SoFiA targeted searches are complete above an integrated HI flux of 0.24 mJy MHz (240 Jy Hz), while we have not been able to determine the completeness limit for SoFiA blind searches in the same range. In order to observe galaxies which have no previous redshift measurements, we will have to include blind searches by eye as well as automated searches.